



The evaluation of plasma electrolytic oxidation properties on car compartments made with Mg alloy

S. Safari^{1*}, M. Nouripour², A. Moshki³, H. Safari⁴

¹ Department of Materials Science and Engineering, Sharif University of Technology/ Engine assembly engineering division, Iran Khodro Co., saeed.safari25@sharif.ir

² Department of Materials Science and Engineering, Sharif University of Technology, m.nouripour16@sharif.ir

³ Department of Mechanical Engineering, Tehran University/ Engine assembly engineering division, Iran Khodro Co., a.moshki@ut.ac.ir

⁴ Department of Mechanical Engineering, Islamic Azad University, hosseinsafari.mech@gmail.com

*Corresponding Author

ARTICLE INFO

Article history:

Received: 5 May 2022

Accepted: 5 September 2022

Keywords:

Plasma electrolytic oxidation

Magnesium alloy

Piston

Corrosion

ABSTRACT

In recent years, the automotive industry has expanded its usage of magnesium alloys because to their favorable metallurgical properties. It is, however, vital to coat the magnesium components like piston in the car engines because of their harsh working environment. In this study, beyond the introduction of novel plasma electrolytic oxidation coating for AZ31 Mg alloy, the metallurgical characteristics of coating generated in silicate and aluminate electrolytes are also examined. Phase studies revealed that along with the presence of MgF_2 and MgO in both coating, Mg_2SiO_4 and $MgAl_2O_4$ were discovered in coatings created in silicate and aluminate electrolytes, respectively. The application of PEO resulted in a considerable drop in corrosion rate, such that the corrosion rate of the coating formed in silicate electrolyte is 2.24×10^{-6} A.cm⁻² and that of the coating created in aluminate electrolyte is 9.5×10^{-7} A.cm⁻², which are 30 and 68 times lower than the rate of uncoated samples, respectively. Additionally, as compared to the uncoated sample, the coating enhances the surface electrical resistance by 72 and 94 times. The microscopic analysis showed that the average diameter of porosities in PEO coating made by silicate electrolyte is higher than that of coating made by aluminate electrolyte.



© Iranian Society of Engine (ISE), all rights reserved.

1) Introduction

The increasing usage of fossil fuels, combined with the increased amount of hazardous emissions produced by their combustion, has made it critical in past few decades to find solutions to minimize fossil fuel consumption. In this context, methods for utilizing alternative energy sources and lightening a variety of vehicles, including automobiles, trains, aircraft, and ships, have been discussed. As a result, the development of new alloys with the goal of reducing weight and enhancing quality in accordance with Fig. 1 has been of great interest and a significant point of evolution in the automobile industry during the last decades. For instance, Volkswagen and Audi introduced a project named a car that consumes less than 3 liters of gasoline per 100 kilometers, with the primary objective of replacing steel and cast iron components with aluminum and magnesium and polymers [1-4].

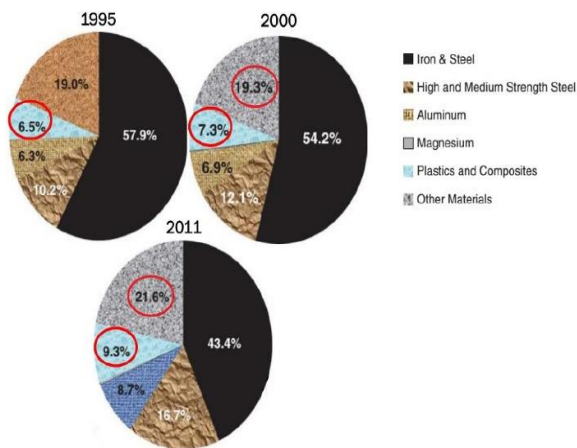


Figure 1: The pie charts of consuming engineering materials over three decades

In general, there are three major issues in the design and construction of automotive components, including friction, heat, and corrosion, which necessitate the use of a range of coatings on various parts of the car. These issues may be addressed and the life of components such as motor pistons extended by applying protective coatings [5]. Nowadays, domestic automobile manufacturers such as Iran Khodro employ the hard anodizing coating process to coat aluminum pistons, which is considered an outdated technique that is not environmentally friendly owing to the nature of the process and the materials used. Additionally, the resulting coating is generally of poor quality, as illustrated in Fig. 2 by the

macroscopic image of the TU5 engine piston crown following an 8-minute hot test.

Magnesium alloys are being employed in the fabrication of a variety of automotive components, such as engine block, cylinder head, Intake manifold, pistons, by significant vehicle companies like GM, Dodge, Honda Motor, Ford, BMW and Alfa Romeo, due to its superior qualities, which include low density, a high specific strength ratio, a low melting temperature, good casting ability, and ease of machining (Fig. 3). By and large, the usage of these alloys results in decreased fuel consumption and production costs.

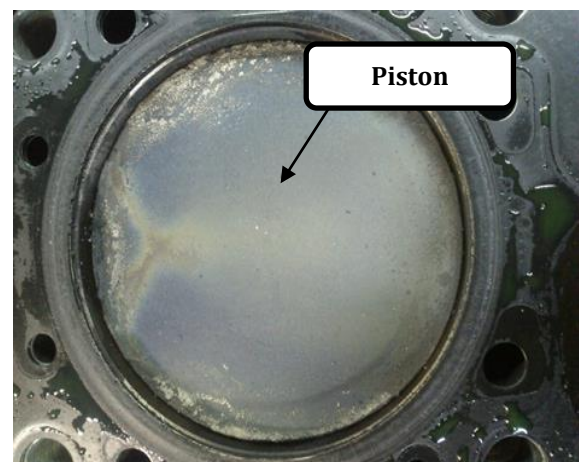


Figure 2: The macroscopic photograph of TU5 engine piston after hot test

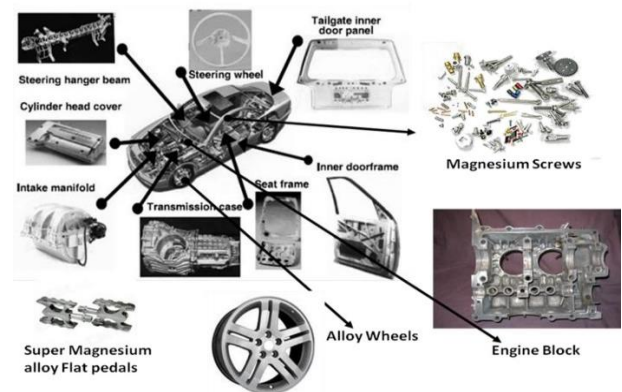


Figure 3: Different compartments of cars which can be made with Mg alloys [3]

There are different ways to modify of Mg properties. For example, magnesium pistons are coated in a relatively advanced method of plasma electrolytic oxidation (PEO) at the end of the manufacturing process. The PEO process is an electrochemical surface treatment that is applied to magnesium and other light metals such as aluminum, titanium, and others in

order to form a thick oxide layer with high corrosion resistance and wear resistance on the surface. It also is significantly more desired than hard anodizing and is also a more environmentally friendly process, as it contains no toxic ingredients to the environment [6-9]. Yet, different researchers have proposed distinct mechanisms for PEO, which is why the process is referred to by a variety of nomenclature, including Micro-Arc oxidation, Anode Spark Electrolysis, Plasma Electrolytic Anode Treatment, and Plasma-Electrolytic Anodizing [5]. The schematic of the PEO process mechanism depicted in Fig. 4 is widely recognized by researchers. At the start of the process and at low voltages, the kinetics of electrode reactions follow Faraday's law. As a result, increasing the voltage results in an increase in current. Finally, the increase in current is constrained by the gas layer released by the electrochemical reactions occurring on the anode surface. In areas where the electrode remains in contact with the electrolyte, the current density continuously increases, causing the electrolyte to boil locally in the adjacent electrode, and once the electrode is completely covered by a continuous layer of low-conductivity gas, almost all electrolysis voltage drops in this thin layer of insulation and near the electrode. As a result, the electric field intensity in this area reaches approximately 10^7 volts per meter, and when an electric field of this magnitude is produced, the gas bubbles are ionized and plasma discharge is performed, resulting in a PEO coating on the surface [10-14].

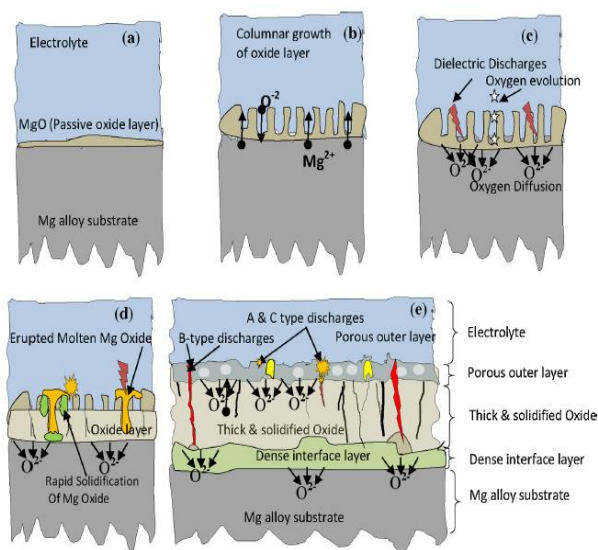


Figure 4: Schematic of the coating formation during PEO process [14]

The goal of this study is to first apply a defect-free PEO coating made of silicate and aluminate electrolytes to a piece of Mg alloy substrate, followed by an examination of the PEO coatings' various features and quality. The coating's formation mechanism (V-t curve), phase analysis, corrosion characteristics, hardness, electrical resistance, and surface morphology have all been investigated.

2) Materials and Methods

In this study, the characteristics of PEO coating applied on the substrate of AZ31 magnesium alloy were investigated, and the chemical composition of this alloy is shown in Table 1.

Table 1: Chemical composition of AZ31 Mg alloy sample (wt %)

Elements	Al	Zn	Mn	Si	Fe	Mg
Percentage	2.77	0.9	0.41	0.01	0.008	Bal.

Substrate samples with a thickness of 2.5 mm were initially cut to dimensions of 20 mm × 40 mm and then prepared and degreased with acetone before coating. Two different electrolytes, silicate and aluminate, were used to apply the PEO coating, the chemical compositions of which are listed in Table 2. Then, in 8.5 minutes, the surface was coated with constant current using a bi-polar pulsed DC and the operating parameters listed in Table 3. Notably, three samples were coated to verify the repeatability of coating method under each condition. Besides, it should be emphasized that the device recorded the voltage every second in order to plot the voltage curve versus the PEO process time [25,26].

The thickness was determined non-destructively using a Fisher thickness meter Dual Scope MP40 model, and then the phases formed during the coating process were studied using an X-ray diffraction (XRD) test with a Philips-XRG3100 device.

Table 2: Chemical composition of Silicate and Aluminate electrolyte

Type of electrolyte	Chemical composition (g/lit)			
	Na ₂ SiO ₃	NaAlO ₂	KOH	NaF
Silicate electrolyte	10	0	2	1.5
Aluminate electrolyte	0	10	2	1.5

Table 3: The PEO process parameters

Duty cycle (%)	frequency (Hz)	Current density (mA/cm ²)
50	50	450

The potentiodynamic polarization test was utilized to investigate the corrosion behavior of the coating and to determine its corrosion rate and electrical resistance. This test was conducted using an Autolab PGSTAT 302N in a 3.5 percent NaCl solution (seawater simulator). In this test, based on ASTM G5-14, the counter electrode, reference electrode, and working electrode were 316 stainless steel, Saturated Calomel Electrode (SCE), and test samples, respectively. The range of applied potential was ± 400 mv relative to Open Circuit potential (OCP), and the scanning voltage rate was 5 mv/sec. Microhardness test was also performed on samples using a Leitz hardness tester in accordance with the ASTM E384-17 standard. Finally, the morphology and shape of the PEO coating were studied using the MIRA3 TESCAN-XMU scanning electron microscope.

3) Results and discussion

3-1) Measurement of PEO coating thickness

The thickness of the PEO coating formed on the magnesium substrate in silicate and aluminate electrolytes over an 8.5-minute period is listed in Table 4. As can be observed, the coating thickness is nearly uniform throughout the sample. Additionally, the silicate electrolyte has a thicker PEO coating than the aluminate electrolyte.

It should be noted that using a non-destructive approach to determine the thickness of PEO coatings is acceptable as long as the coating thickness is less than 40 μm ; however, if the coating thickness exceeds 40 μm , this method should not be used. It makes little sense due to its numerous faults [15].

Table 4: Thickness of PEO coating formed in different electrolytes

Type of electrolyte	Average coating thickness (μm)
Silicate electrolyte	20.36 ± 0.52
Aluminate electrolyte	17.13 ± 0.17

In addition, the thickness of the coating is calculated using a microscopic image of the cross section of the coated samples. Using the MIP software, the thickness of the coating produced in the silicate electrolyte according to Fig. 5 is determined to be 19.96 ± 1.26 μm . With respect to Fig. 6, the coating created in the aluminate electrolyte has a thickness of 14.4 ± 1.83 μm . It is evident that these two

methods for measuring the thickness yielded slightly different results, which may be negligible.

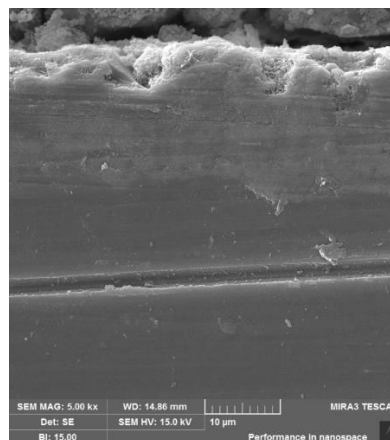


Figure 5: SEM images of PEO coating formed in Silicate electrolyte cross section

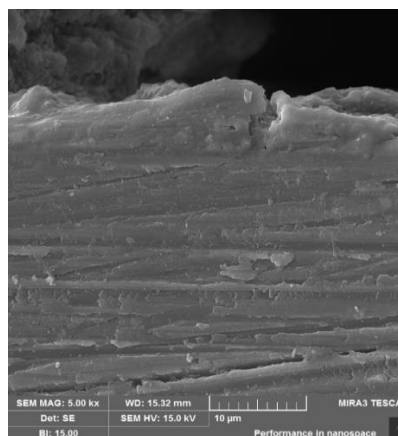


Figure 6: SEM images of PEO coating formed in Aluminate electrolyte cross section

3-2) V-t curve in PEO process

The voltage-time curves of the sample coated in silicate and aluminate electrolytes are shown in Fig. 7 together with guide lines dividing the various stages. As one can see, the voltage changes linearly with a steep slope over time in the first stage, but no spark was created on the sample surface, as represented in Fig. 8 and 9. The sharp slope of the first stage curve can be explained by two phenomena: first, the dissolution of the substrate results in the formation of a passive layer with low electrical conductivity on the surface; and second, a large volume of gas is released at this stage, some of which is absorbed by the anode surface. Due to the presence of these two layers with extremely low electrical conductivity, the voltage must rise rapidly to maintain a constant current density [14-16].

The voltage continues to climb linearly with time in the second stage of the process, although the slope of these increases drops significantly. At this stage in which the starting voltage is referred to as the breakdown voltage [14-16], very small white sparks are visible on the surface of the sample, which sweeps the anode surface rapidly. The shape, size, and color of the sparks generated at this stage are distinct from those generated during the other stages.

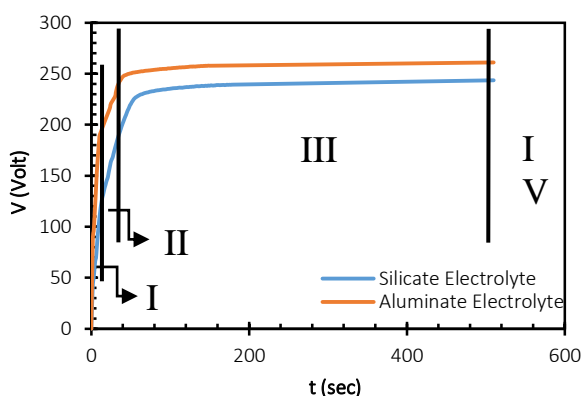


Figure 7: Voltage-time curves during PEO of AZ31 for 510 seconds at $450 \text{ mA}\cdot\text{cm}^{-2}$ in Silicate and Aluminate electrolyte

By the third stage, the quantity of sparks has been gradually decreased but their size has been grown [17,18]. According to Fig. 7 and 8, the color of the sparks also changes in this stage in comparison to the previous stage. Furthermore, the magnitude of the voltage changes over time drops dramatically at this stage, and the slope of the curve begins to climb gently, in contrast to the previous stages. The reason is the oxide coating has completely covered the surface and the surface resistance has attained a constant value, and the thickness of coating is increased only during this step. These observations contrast sharply with the first and second stages, in which the voltage increases dramatically by forming an early oxide layer to maintain current density at a constant level throughout the process.

In this research, the process comes to a halt practically immediately upon entering the fourth stage, but in general, during the fourth stage, only a few massive and high-energy sparks are produced on the surface of the sample in preferred and particular locations. Sparks might degrade the coating's quality and cause irreversible harm. As a result, as

previously stated, it is recommended not to enter this stage of the coating process. It is worth mentioning after a long period of time, the voltage declines, and a portion of the oxide coating formed during the PEO process dissolves, resulting in a decrease in electrolyte conductivity [18].

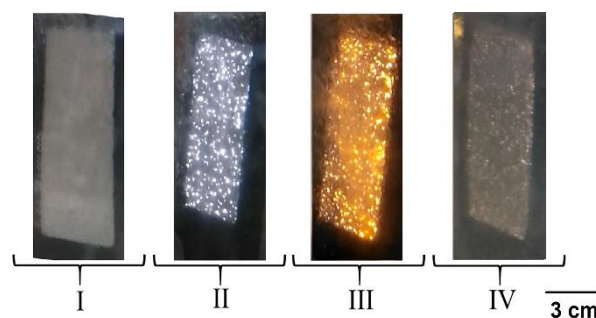


Figure 8: The macroscopic photographs of sample surface at different stage of the PEO process in Silicate electrolyte; I) gas released II) very small white sparks created III) sparks color change to orange IV) large sparks in preferred location

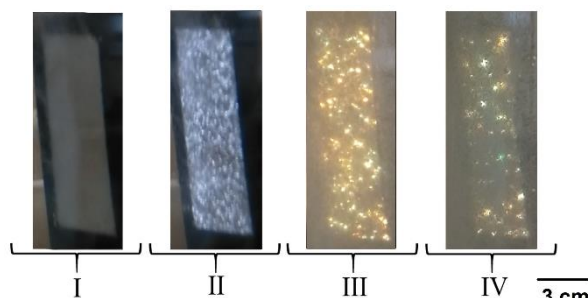


Figure 9: The macroscopic photographs of sample surface at different stage of the PEO process in Aluminate electrolyte; I) gas released II) very small white sparks created III) sparks color change to green/orange IV) large sparks in preferred location

3-3) Phase studies

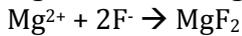
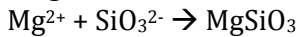
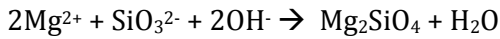
The XRD analysis of the sample coated with silicate electrolyte is shown in Fig. 10, indicating that phases such as MgO , Mg_2SiO_4 , and MgF_2 are produced on the surface during the PEO process.

The reactions that result in the production of these phases in the surface coating are as follows:



It should be highlighted that the production of oxide films on Mg is caused by the outward diffusion of Mg ions, whereas high voltage has an effect on the inward diffusion of SiO_2^{3-} , OH^- , and F^- ions. When the concentration of these ions reaches a critical amount at the electrode-electrolyte interface, coating formation

reactions occur, justifying the creation of the aforementioned phases [19-21].



And the MgO phase is formed according to the following reactions: [19-21].

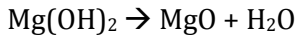
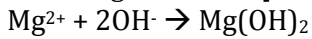
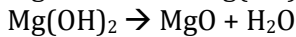
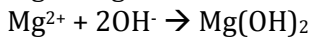


Fig. 10 also shows the X-ray diffraction pattern of the sample coated with aluminate electrolyte. As can be seen, throughout the PEO process, phases like as MgO, MgAl₂O₄, and MgF₂ are produced on the surface.

The reactions that result in the development of these phases in the surface coating are as follows: [21-23].



The following reactions result in the formation of Al₂O₃ via the sparking process at high temperatures, followed by a reaction with MgO, which results in the production of the MgAl₂O₄ phase. Subsequently, by increasing the sodium aluminate concentration in the electrolyte, the conditions for the creation of additional MgAl₂O₄ are provided [21-23].

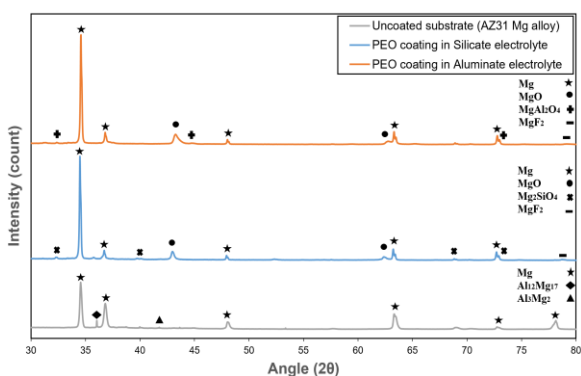
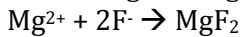
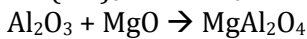
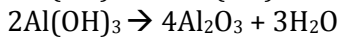
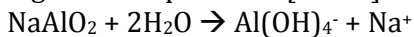


Figure 10: X-ray diffraction pattern of AZ31 magnesium alloy and PEO coating formed in Silicate and Aluminate electrolytes

3-4) Corrosion behavior investigation

Fig. 11 illustrates the polarization curves of coated and untreated samples. Table 5 also includes electrochemical data acquired from these curves, including as corrosion rate,

corrosion potential, and electrical resistance for all samples.

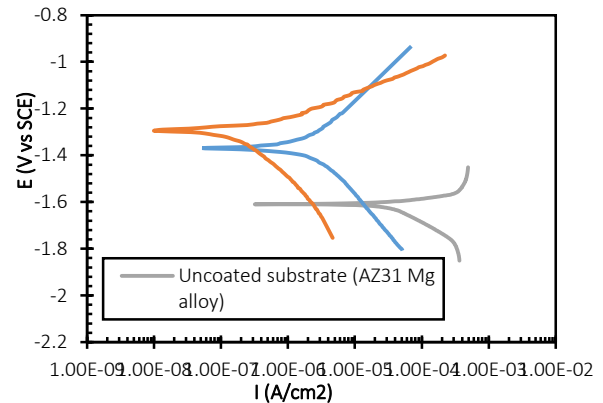


Figure 11: Potentiodynamic polarisation curves of the samples in the 3.5 % NaCl solution

As presented in Fig. 10 and Table 5, the corrosion rate (I_{corr}) is considerably lower in samples with PEO coating than in the other without coating, indicating the importance of the coating. During this coating process, a thick oxide layer is formed on the surface, considerably increasing the surface's corrosion resistance. Because in general, this oxide layer almost disconnects the corrosive environment from the sample surface. Therefore, anodic and cathodic reactions are delayed and the corrosion rate is minimized. It is also found that the corrosion potential of surfaces with protective coating tends to more noble potentials, which also reflects a decrease in the surface tendency to corrosion. However, it should be noted that the PEO coating is porous and contains tiny fissures, such that corrosive solutions can penetrate the coating surface and reach the substrate surface, causing anodic and cathodic reactions and corrosion-induced surface products [24]. While continuing to increase the current density and coating time expands the coating thickness, it also increases the coating's porosity and surface roughness, resulting in a loss in wear and corrosion resistance [25-26].

Previous studies have reported that plasma electrolytic oxidation is a technique that can be repeated, and that its coating quality is much superior than that of anodizing coatings. Subsequently, the corrosion rate of the sample produced by the second approach is nearly double that of the first, and the wear resistance of the PEO coating is also higher [27-29].

Magnesium corrosion is largely insensitive to oxygen levels in aqueous environments due to the electrochemical interaction that produces magnesium hydroxide and hydrogen gas during magnesium dissolution. However, oxygen is a major component in atmospheric corrosion. Corrosion partial reactions are as follows: [33-35].

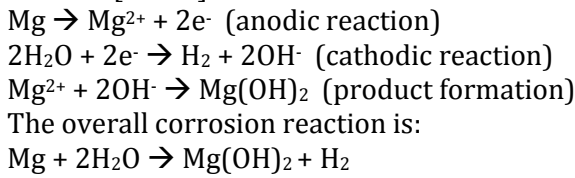


Table 5: Potentiodynamic polarisation data of substrate and PEO coating in Silicate and Aluminate electrolyte

Samples	b_a V/dec	$-b_c$ V/dec	E_{corr} V	R_p $\Omega \cdot \text{cm}^2$	I_{corr} A/cm ²
Uncoated	0.07	0.3	-1.61	359	6.55×10^{-5}
PEO/Silicate electrolyte	0.3	0.29	-1.37	26005	2.24×10^{-6}
PEO/Aluminate electrolyte	0.1	0.29	-1.29	34039	9.5×10^{-7}

Fig. 12 shows a microscopic image of the surface corrosion of the uncoated Mg alloy sample after immersion in a 3.5 NaCl solution for 15 minutes. The regional EDS analysis can be seen in Table 6, where the high percentage of oxygen indicates the corrosion reactions and the formation of oxide compounds such as MgO on the surface.

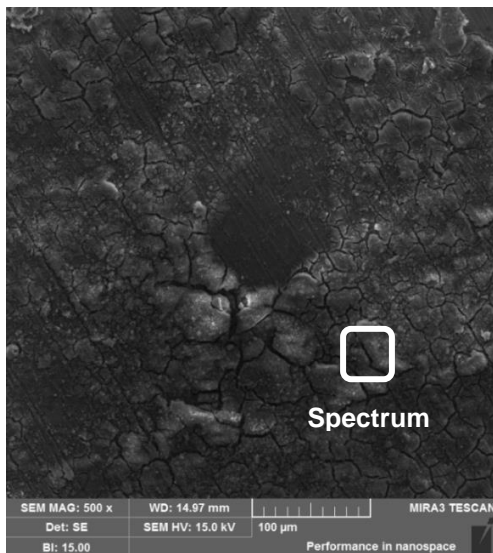


Figure 12: SEM image of corrosion of magnesium sample without protective PEO coating

Table 6: Data obtained from EDS test performed in corroded zones

Area	Wt.%				
	Mg	Al	O	Cl	Zn
Spectrum	38.5	2.8	52.1	6.3	0.3

Due to the porous of the PEO coating, it is feasible for the corrosive solution to penetrate the coating and reach the substrate after an extended length of time, as depicted in the schematic Fig. 13. [24]

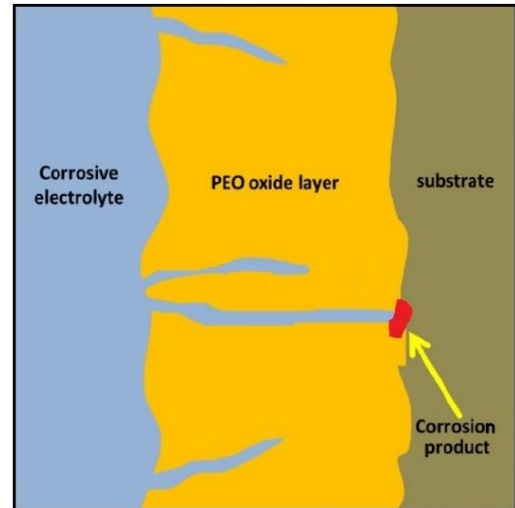


Figure 13: Schematic of PEO coating on magnesium immersed in 3.5 wt% NaCl solution [24]

Corrosion reactions of sample with PEO coating are as follows: [34,35]

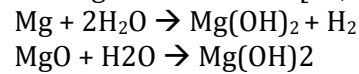


Fig. 14 and 15 are microscopic views of coated samples immersed in a corrosive solution of 3.5% NaCl, which, unlike Fig. 12, do not demonstrate considerable surface damage, indicating the coating's role and quality.

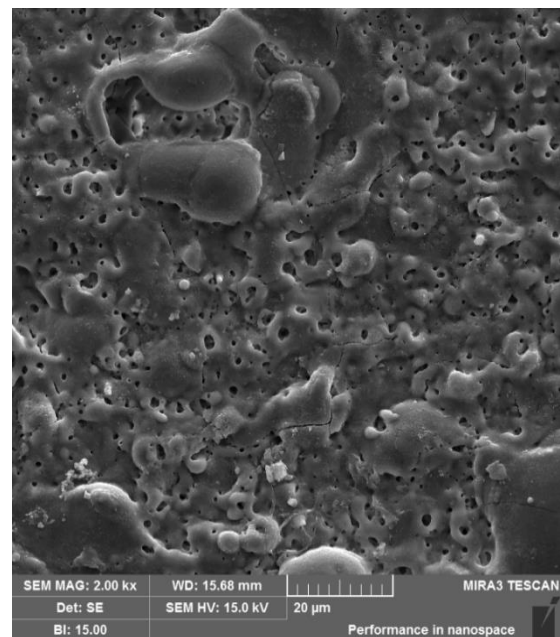


Figure 14: SEM image of corrosion of PEO coating formed in Silicate electrolyte

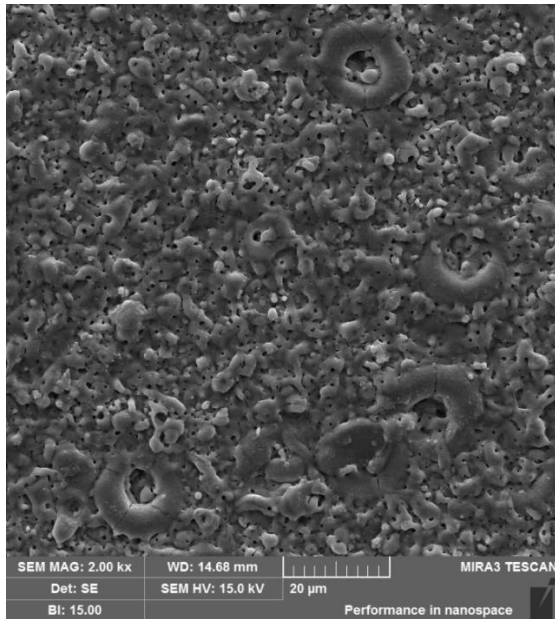


Figure 15: SEM image of corrosion of PEO coating formed in Aluminate electrolyte

As shown in Table 5, the electrical resistance of the substrate surface rises substantially as a result of the presence of a thick oxide coating. This effect results in a dramatic decrease in thermal conductivity, such that the thermal conductivity of the uncoated AZ31 Mg alloy sample increases from 96.23 W/mK to roughly 2-4 W/mK in the PEO-coated sample, according to the studies published earlier [30-31]. This demonstrates the exceptional thermal barrier provided by this type of coating, which is beneficial when used as a protective piston coating.

3-5) Hardness

Table 7 lists the average hardness of uncoated mg alloy substrate and samples coated with silicate and aluminate electrolytes. According to this table, the hardness of the surface significantly increases after the production of the PEO coating, demonstrating the importance of the oxide layer formed on the surface. It is reported that under certain conditions and with the addition of nanoparticles to the PEO coating as a filler, its hardness can be boosted to above 1000 Vickers [36].

Table 7: Hardness of PEO coating formed in different electrolytes

Samples	Average hardness (HV)
Uncoated	79 ± 2.7
PEO Coating (Silicate electrolyte)	183 ± 3.9
PEO Coating (Aluminate electrolyte)	226 ± 4.6

3-6) Microscopic examination

In general, PEO coatings comprise of two main layers: an exterior layer with small and large porosities, and an interior layer that is entirely compacted and dense. SEM images of the coating are shown in Fig. 16 and 17. As mentioned previously, the surface of the coating is porous, and the average diameter of the micro-pores was determined using MIP image analysis software. The average diameter of the micro-pores in the coating created in silicate electrolyte is $3.14 \mu\text{m}$, while those in the coating created in aluminate electrolyte is $2.96 \mu\text{m}$.

The magnitude of these porosities can be altered by a variety of factors, including the electrolyte's concentration, the addition of particular additives to the electrolyte, the applied current density, etc. [25,26].

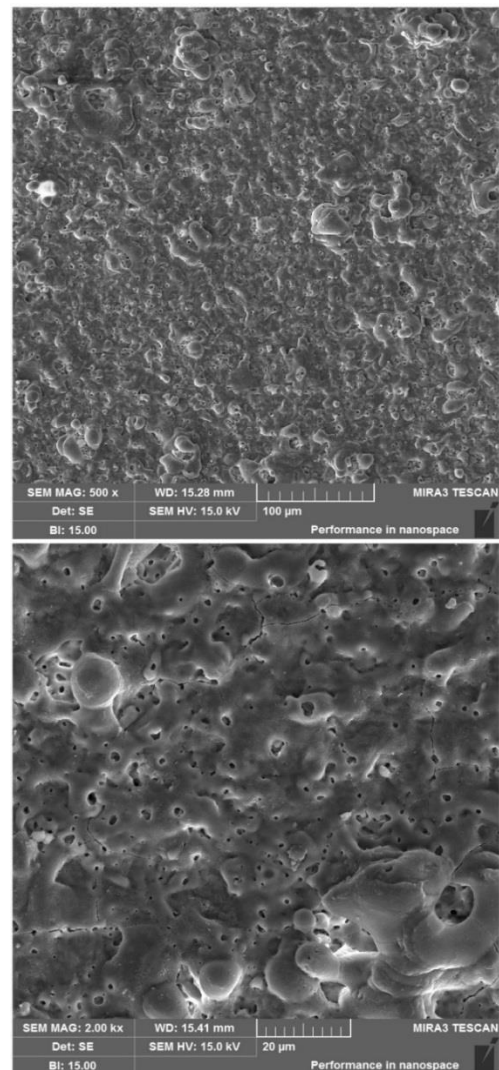


Figure 16: SEM images of surface morphology of PEO coating formed in Silicate electrolyte

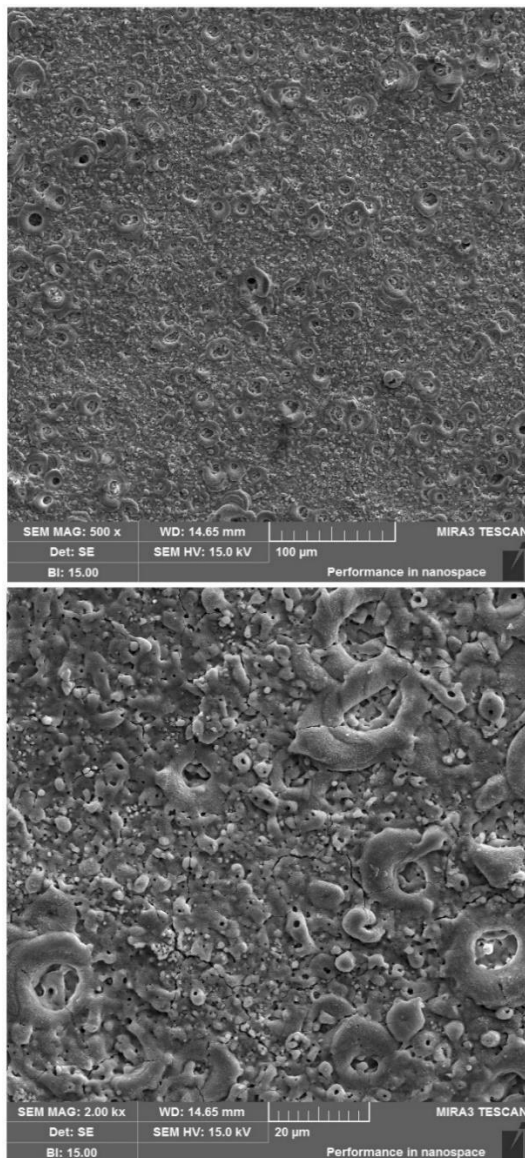


Figure 17: SEM images of surface morphology of PEO coating formed in Aluminate electrolyte

4) Conclusions

In this study, the quality and properties of PEO coatings applied on AZ31 substrates in silicate and aluminate electrolytes are investigated and the following results are obtained.

- 1) According to the V-t curves, the breakdown voltage of coating process in aluminate electrolyte is more than silicate electrolyte, due to lower electrical conductivity of former electrolyte than that of latter one.
- 2) Based on the results of XRD patterns, it can be concluded that PEO coating applied in silicate electrolyte has phases such as MgO, Mg₂SiO₄ and MgF₂, and PEO coating formed in aluminate electrolyte has phases like MgO, MgAl₂O₄ and MgF₂.

3) The corrosion rate of PEO coating created in silicate electrolyte is 2.24×10^{-6} A/cm² and in aluminate electrolyte is 9.5×10^{-7} A/cm², that is 30 and 68 times less than that of uncoated sample.

4) The surface hardness from 79 HV in the uncoated sample increases to 183 HV and 226 HV in the samples coated in silicate and aluminate electrolytes, respectively.

5) The results of morphology analysis indicate that the average diameter of porosities in the coating created in silicate electrolyte is 3.14 μm and the coating formed in aluminate electrolyte is 2.96 μm.

5) References

- [1] H. Friedrich, S. Schumann, "Research for a new age of magnesium in the automotive industry", *Journal of material processing technology*, vol.117, pp.276-281, 2001.
- [2] M. K. Kulekci, "Magnesium and its alloys applications in automotive industry", *The International Journal of Advanced Manufacturing Technology*, Vol.39, pp.851-865, 2008.
- [3] D. S. Kumar, C. T. Sasanka, K. Ravindra, K. N. S. Suman. "Magnesium and its alloys in automotive applications—a review", *Journal of Material Science and Technology*, Vol.4, pp.12-30, 2015.
- [4] M. Yeganeh, N. Mohammadi, "Superhydrophobic surface of Mg alloys: A review", *Journal of magnesium and alloys*, Vol.6, pp.59-70, 2018.
- [5] H. Yamagata, "The Science and Technology of Materials in Automotive Engines", Woodhead Publishing, 2005.
- [6] J. Tan, Jovan, S. Ramakrishna, "Applications of magnesium and its alloys: A review", *Applied Sciences*, Vol.11, pp.61-68, 2021.
- [7] J. Wang, X. Pang, H. Jahed. "Surface protection of Mg alloys in automotive applications: A review", *AIMS Materials Science*, Vol.6, pp.567-600, 2019.
- [8] H. Dong, "Surface Engineering of Light Alloys Aluminium, Magnesium and Titanium Alloys", Woodhead Publishing, 2010.
- [9] Gh. Barati, M. Aliofkhaezrai, P. Hamghalam, N. Valizade, "Plasma electrolytic oxidation of magnesium and its alloys: Mechanism, properties and applications", *Journal of Magnesium and Alloys*, Vol.5, pp. 74-132, 2017.

- [10] A. L. Yerokhin, X. Nie, "Plasma electrolysis for surface engineering", *Surface and Coatings Technology*, Vol.122, pp.73-93, 1999.
- [11] F. Simchen, S. Maximilian, A. Kopp, T. Lampke, "Introduction to plasma electrolytic oxidation—An overview of the process and applications", *Coatings*, Vol.10, pp.628-646, 2020.
- [12] M. Kaseem, S. Fatimah, N. Nashrah, Y. Gun Ko, "Recent progress in surface modification of metals coated by plasma electrolytic oxidation: Principle, structure, and performance", *Progress in Materials Science*, Vol.117, 2021.
- [13] P. Gupta, G. Tenhundfeld, E. O. Daigle, D. Ryabkov, "Electrolytic plasma technology: Science and engineering - An overview", *Surface and Coatings Technology*, Vol.201, pp.8746-8760, 2007.
- [14] R. O. Hussein, X. Nie, D. O. Northwood, "An investigation of ceramic coating growth mechanisms in plasma electrolytic oxidation (PEO) processing", *Electrochimica Acta*, Vol.112, pp.111-119, 2013.
- [15] S. Aliasghari, P. Skeldon, G. E. Thompson, "Plasma electrolytic oxidation of titanium in a phosphate/silicate electrolyte and tribological performance of the coatings", *Applied Surface Science*, Vol.316, pp.436-476, 2014.
- [16] S. Onoa, S. Moronukia, Y. Morib, "Effect of electrolyte concentration on the structure and corrosion resistance of anodic Films formed on Magnesium through plasma electrolytic pxdation", *Electrochimica Acta*, Vol.240, pp.415-423, 2017.
- [17] Z. Qiu, R. Wang, Y. Zhang, "Study of Coating Growth Behavior During the Plasma Electrolytic Oxidation of Magnesium Alloy ZK60", *Journal of Materials Engineering and Performance*, Vol.24, pp.1483-1491, 2015.
- [18] W. C. Gu, G. H. Lv, H. Chen, G. L. Chen, "Characterisation of ceramic coatings produced by plasma electrolytic oxidation of aluminum alloy", *Materials Science and Engineering*, Vol.447, PP.158-162, 2007.
- [19] H. Duan, Ch. Yan, F. Wang, "Growth process of plasma electrolytic oxidation films formed on magnesium alloy AZ91D in silicate solution", *Electrochimica Acta*, Vol.52, pp.5002-5009, 2007.
- [20] D. Sreekanth, K. V. Warlu, N. Rameshbabu, "Effect of various additives on morphology and corrosion behavior of ceramic coatings developed on AZ31 magnesium alloy by plasma electrolytic oxidation", *Ceramics International*, Vol.38, pp.4607-4615, 2011.
- [21] A. Ghasemi, V. S. Raja, C. Blawert, W. Dietzel, K. U. Kainer. "The role of anions in the formation and corrosion resistance of the plasma electrolytic oxidation coatings", *Surface and Coatings Technology*, Vol.204, pp.1469-1478, 2010.
- [22] Y. Ma, X. Nie, D. O. Northwood, H. Hu, "Systematic study of the electrolytic plasma oxidation process on a Mg alloy for corrosion protection", *Thin Solid Films*, Vol.494, pp.296-301, 2006.
- [23] L. S. Wang, C. X. Pan, "Characterisation of microdischarge evolution and coating morphology transition in plasma electrolytic oxidation of magnesium alloy", *Surface engineering*, Vol.23, pp.324-328, 2007.
- [24] G. A. Mengesha, J. P. Chu, B. S. Lou, J. W. Lee. "Corrosion performance of plasma electrolytic oxidation grown oxide coating on pure aluminum: effect of borax concentration", *Journal of Materials Research and Technology*, Vol.9, pp.8766-8779, 2020.
- [25] X. Li, X. Y. Liu, B. L. Luan, "Corrosion and wear properties of PEO coatings formed on AM60B alloy in NaAlO₂ electrolytes", *Applied surface science*, Vol.257, pp.9135-9141, 2011.
- [26] J. J. Zhuang, R. G. Song, N. Xiang, Y. Xiong, Q. Hu, "Effect of current density on microstructure and properties of PEO ceramic coatings on magnesium alloy", *Surface Engineering*, Vol.33, pp.744-752, 2017.
- [27] S. Rahimi, A. Bordbar Khiabani, B. Yarmand, A. Kolahi, "Comparison of corrosion and antibacterial properties of Al alloy treated by plasma electrolytic oxidation and anodizing methods", *Materials Today: Proceedings*, Vol.7, pp. 1567-1576, 2018.
- [28] S. Viswanathan, "Superhydrophobic surfaces and coatings by electrochemical anodic oxidation and plasma electrolytic oxidation", *Advances in Colloid and Interface Science*, Vol.283, pp. 234-245, 2020.
- [29] Y. Rao, Q. Wang, J. Chen, C. Ramachandran, "Abrasion, sliding wear, corrosion, and cavitation erosion characteristics of a duplex coating formed on AZ31 Mg alloy by sequential application of cold spray and plasma electrolytic oxidation techniques", *Materials Today Communications*, Vol.26, pp.947-978, 2021.
- [30] J. A. Curran, T. W. Clyne, "The thermal conductivity of plasma electrolytic oxide coatings on aluminium and magnesium", *Surface and Coatings Technology*, Vol.199, pp.177-183, 2005.

- [31] J. A. Curran, H. Kalkancı, Y. Magurova, T. W. Clyne, "Mullite-rich plasma electrolytic oxide coatings for thermal barrier applications", *Surface and Coatings Technology*, Vol. 201, pp.8683-8687, 2007.
- [32] E. Ramakrishnan, C. Premchand, P. Manojkumar, N. Rameshbabu, "Development of thermal control coatings on AA7075 by plasma electrolytic oxidation (PEO) process", *Materials Today: Proceedings*, Vol. 46, pp.1085-1093, 2021.
- [33] G. L. Song, A. Atrens, "Corrosion Mechanisms of Magnesium", *Advanced Engineering Materials*, Vol.1, pp.11-33,1999.
- [34] H. Duan, K. Du, Ch. Yan, F. Wang, "Electrochemical corrosion behavior of composite coatings of sealed MAO film on magnesium alloy AZ91D", *Electrochimica Acta*, Vol.51, pp.2898-2908, 2006.
- [35] L. Pezzato, L. Bertolucci, R. Bertolini, A. G. Settimi, K. Brunelli, M. Olivier, M. Dabalà. "Corrosion and mechanical properties of plasma electrolytic oxidation-coated AZ80 magnesium alloy", *Materials and Corrosion*, Vol.70, pp.2103-2112. 2019.
- [36] G. Rapheal, S. Kumar, C. Blawert, N. B. Dahotre, "Wear behavior of plasma electrolytic oxidation (PEO) and hybrid coatings of PEO and laser on MRI 230D magnesium alloy", *Wear*, Vol.271, pp.1987-1997, 2011.



فصلنامه علمی تحقیقات موتور

تارنمای فصلنامه: www.engineersearch.ir

DOI:10.22034/ER.2022.697929



ارزیابی خواص پوشش اکسیدی پلاسمای الکترولیتی اعمالی روی قطعات منیزیمی خودرو

سعید صفری^{۱*}، محمد حسین نوری پور^۲، علیرضا مشکی^۳، حسین صفری^۴

^۱ فارغ التحصیل کارشناسی ارشد، دانشکده مهندسی و علم مواد، دانشگاه صنعتی شریف/ مهندس اداره مهندسی مونتاژ موتور، شرکت ایران خودرو، saeed.safari25@sharif.ir

^۲ فارغ التحصیل کارشناسی ارشد، دانشکده مهندسی و علم مواد، دانشگاه صنعتی شریف، m.nouripour16@sharif.ir

^۳ فارغ التحصیل کارشناسی ارشد، دانشکده مکانیک، دانشکدگان فنی دانشگاه تهران/ مهندس اداره مهندسی مونتاژ موتور، شرکت ایران خودرو، a.moshki@ut.ac.ir

^۴ فارغ التحصیل کارشناسی، دانشکده مهندسی مکانیک، دانشگاه آزاد اسلامی، hosseinsafari.mech@gmail.com

* نویسنده مسئول

اطلاعات مقاله

تاریخچه مقاله:

دریافت: ۱۵ اردیبهشت ۱۴۰۱

پذیرش: ۱۴ شهریور ۱۴۰۱

کلیدواژه‌ها:

اکسیداسیون پلاسمای الکترولیتی

آلیاژ منیزیم

پیستون

خوردگی

چکیده

در سال‌های اخیر استفاده از آلیاژهای منیزیم در صنعت خودروسازی به جهت خواص متالورژیکی مطلوب افزایش پیدا کرده است. اعمال پوشش بر روی قطعات منیزیمی به‌کاررفته در موتور خودرو نظیر پیستون با در نظر گرفتن شرایط کاری شدید آن‌ها الزامی می‌باشد. در این پژوهش، ابتدا پوشش مدرن اکسیداسیون پلاسمای الکترولیتی معرفی می‌شود و در ادامه خواص متالورژیکی پوشش ایجادشده بر روی آلیاژ AZ31 در الکترولیت‌های سیلیکاتی و آلومیناتی مورد بررسی و مقایسه قرار می‌گیرد. نتایج حاصل از مطالعات فازی بر روی پوشش‌ها نشان داد علاوه بر حضور فازهای MgO و MgF_2 در هر دو پوشش، فازهای Mg_2SiO_4 و $MgAl_2O_4$ به ترتیب در پوشش‌های ایجادشده از الکترولیت سیلیکاتی و آلومیناتی وجود دارند. اعمال پوشش PEO منجر به کاهش قابل توجه سرعت خوردگی می‌شود. سرعت خوردگی پوشش ایجاد شده در الکترولیت سیلیکاتی $2/24 \times 10^{-6} \text{ A.cm}^{-2}$ و در الکترولیت آلومیناتی $9/5 \times 10^{-7} \text{ A.cm}^{-2}$ می‌باشد که به ترتیب ۳۰ و ۶۸ برابر نسبت نمونه فاقد پوشش کمتر است. همچنین اعمال پوشش منجر به افزایش ۷۲ و ۹۴ برابری مقاومت الکتریکی سطح نسبت به نمونه فاقد پوشش می‌شود. بررسی میکروسکوپی نیز نشان داد که قطر متوسط تخلخل‌ها در پوشش PEO ایجاد شده در الکترولیت سیلیکاتی نسبت به پوشش آلومیناتی بزرگتر است.



تمامی حقوق برای انجمن علمی موتور ایران محفوظ است.